JOURNAL OF VIROLOGY, Nov. 1996, p. 8182–8186 Vol. 70, No. 11
0022-538X/96/$04.00+0

Tandem Mengovirus 5′ Pseudoknots Are Linked to Viral RNA Synthesis, Not Poly(C)-Mediated Virulence

LEE R. MARTIN AND ANN C. PALMENBERG*

Institute for Molecular Virology and Department of Animal Health & Biomedical Sciences, University of Wisconsin—Madison, 1655 Linden Dr., Madison, Wisconsin 53706

Received 15 March 1996/Accepted 25 July 1996

The RNA genomes from the cardioviruses, hepatoviruses, and aphthoviruses encode two to five tandem pseudoknots within their 5′ untranslated regions. These pseudoknots lie adjacent to a pyrimidine-rich sequence, which in cardio- and aphthoviruses takes the form of a homopolymeric poly(C) tract. Seven deletion mutations within mengovirus pseudoknots PK_B and PK_C were created and characterized. When tested in tissue culture, mengovirus genomes with alterations in PK_C were viable but had small plaque phenotypes. Larger plaque revertants were isolated and partially characterized, and each proved to be a second-site pseudorevertant with (unmapped) changes elsewhere in the genome. The infectious PK_C mutant viruses were highly lethal to mice, and deletions in this motif did not affect mengovirus virulence in the same manner as deletions in the adjacent poly(C) tract. In contrast, deletions in PK_B, or deletions which spanned PK_B + PK_C, produced nonviable genomes. Cell-free translations directed by any of the altered PK sequences gave normal polyprotein amounts relative to wild-type mengovirus. But viral RNA accumulation during HeLa cell infection was dramatically impaired, even with the least disruptive of the PK_C changes, suggesting the pseudoknots play an essential though undefined role in RNA synthesis and moreover that an intact PK_B structure is critical to this function.

Mengovirus is a cardiovirus in the picornavirus family. The genome is a positive-sense, single-stranded RNA molecule, identical in organization to that of encephalomyocarditis virus (EMCV). The genome begins with an unusually long 5′ untranslated region (5′ UTR), followed by an open reading frame for the viral polyprotein, and terminates with a short 3′ UTR. As with the genomes from related cardio-, aphtho-, and hepatoviruses, the mengovirus RNA has a distinctive array of secondary and tertiary structural motifs within its 5′ UTR (Fig. 1). The 5′ terminal region is typically modeled with two tandem pseudoknots, PK_B and PK_C, between the extended terminal stem-loop A and the nearby single-stranded, homopolymeric poly(C) tract (6). The hepatoviruses (hepatitis A) are structurally similar to mengovirus in this region except that their poly(C) homologs are somewhat shorter (30 to 50 bases) and very rich with uridine discontinuities (17). The aphthoviruses have the longest poly(C)s; their pseudoknots are located 3′ rather than 5′ to the homopolymer, and moreover their 5′ pseudoknot segments may contain as many as three to five tandemly linked knot elements, depending upon the isolate of virus (4, 9, 15). Within any of these viruses, each pseudoknot requires 18 to 23 nucleotides to form and is usually separated from companion knots by 2 to 5 spacer nucleotides.

Although there is minimal sequence conservation among the 5′ pseudoknots from the different viral genera, or even within knots from related strains (4, 6, 15), their overall topological conservation among these picornaviruses, and its obvious genetic load commitment, suggests these motifs must play some vital role for the virus. In other systems, pseudoknots and related tertiary structures moderate a variety of biological activities, usually functioning as essential regulatory elements for translation initiation, ribosomal frameshifting, ribozyme activity, replication initiation, or genome stability (26). Situated 5′ or 3′ of the viral poly(C), and encoded only within picornaviruses that have these tracts, the 5′ pseudoknot motifs have been logically linked to the functions of the homopolymeric region. It is known that the poly(C) tracts of cardio- and aphthoviruses can be deleted from recombinant constructs without consequence for viral growth in tissue culture. Instead, a poly(C)-dependent phenotype usually becomes apparent only during animal infection. With mengovirus, in particular, the precise poly(C) length plays a critical role in the observation of virulence, and artificial truncation of the tract strongly attenuates mengovirus for virulence (3, 16, 18). Yet, similar poly(C) deletions in EMCV or foot-and-mouth disease virus (an aphthovirus) do not have analogous effects, as these viruses are only partially attenuated by homopolymer truncation (10, 22). Behind our particular interest in the mengovirus pseudoknots was the conjecture that these adjacent 5′ structures might work in concert with the viral poly(C) and perhaps map as part of a larger virulence domain. If so, their various contributions or sequence differences might explain why virus virulence is dissimilarly affected by poly(C) modification in other viruses.

To test this hypothesis, we engineered seven directed mutational disruptions into the pseudoknot sequences of mengovirus cDNAs. The starting plasmid, pMwt, contains a full-length, virulent mengovirus sequence, including the wild-type poly(C) tract of $C_{44}UC_{10}$ (7). Limited reactions with *Bal*31 or mung bean nucleases were initially performed on pMΔ1518-7803, a subclone of pMwt with a unique *Ppu*MI site in the region that encodes PK_C. The plasmid termini were then made blunt with T4 DNA polymerase and religated before amplification of the plasmids in MV1190 bacteria. Transformants were screened by *Ppu*MI digest and dideoxy sequence analysis. Table 1 lists the panel of mutated segments transferred to pMwt contexts. Plasmids pMΔ114, pMΔ114-119, and pMΔ107-139 had 1, 6, and 33 base deletions constrained to PK_C, respectively. Plasmids

* Corresponding author. Mailing address: Dept. of Animal Health & Biomedical Sciences, 1655 Linden Dr., Madison, WI 53706. Phone: (608) 262-7519. Fax: (608) 262-7420. Electronic mail address: Palmenberg@bioinformatics.bocklabs.wisc.edu.

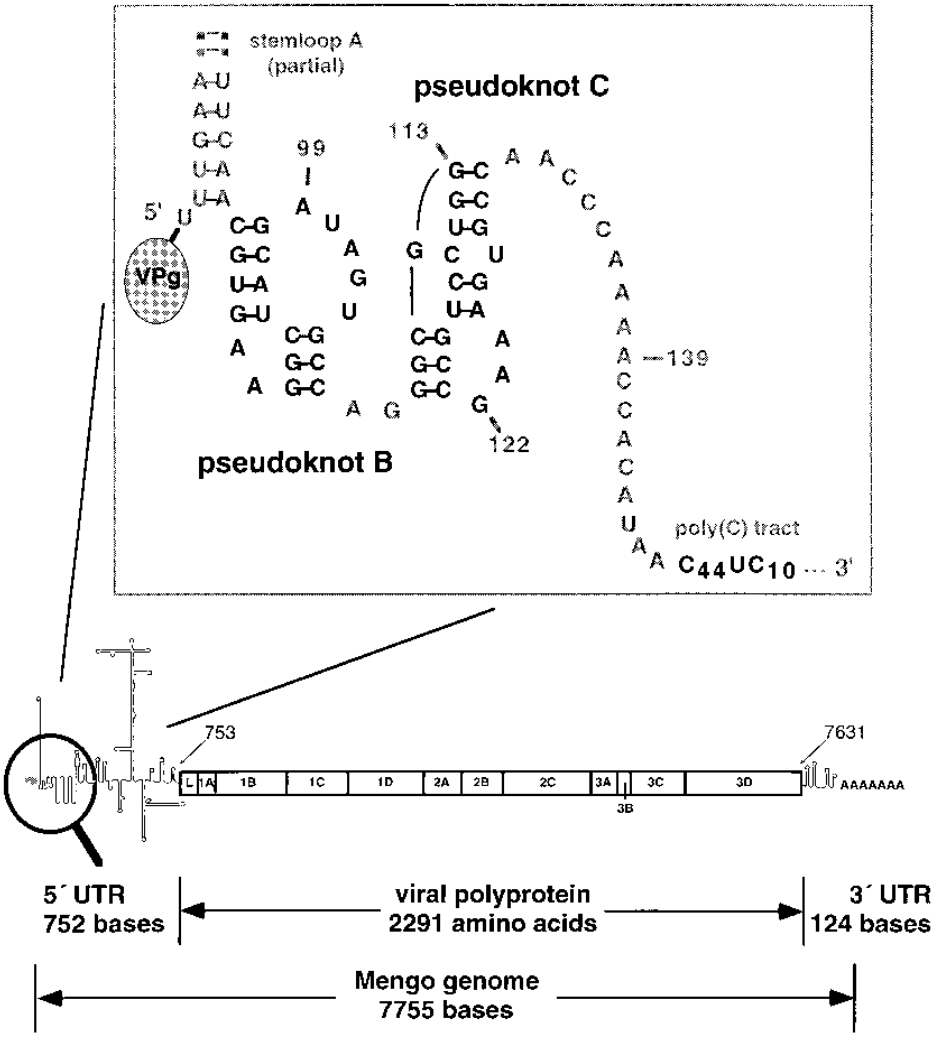

FIG. 1. Schematic representation of the mengovirus genome with an inset of the 5′ UTR pseudoknots. A model was developed after EMCV-R (6) and is consistent with computer-generated optimal and suboptimal energy calculations for the intact genome (25a), chemical and enzymatic probing of EMCV RNA, and sequence conservation among related cardioviruses (6, 19, 28). The two predicted pseudoknots between 5′ terminal stem-loop A and the viral poly(C) tract are designated PK_B and PK_C, respectively. Base numbering is relative to mengovirus M (GenBank no. L22089). The *Ppu*MI site used for mutagenesis extends from base 112 to base 118.

pMΔ99-118 and pMΔ90-144 had 20 and 55 base deletions, respectively, that spanned both pseudoknots. The largest deletion, pMΔ56-134 (79 bases), removed both pseudoknots and also disrupted the base of stem-loop A. Recombinant PCR (14, 25) produced an additional cDNA with a precise deletion of PK_B (20 bases), a mutation not obtainable by the exonuclease method. The mutagenic primer annealed to the 15 bases 5′, and 20 bases 3′, of PK_B but not to the sequences of PK_B itself. After amplification with an outlying 3′ primer, the PCR product was inserted into pBS-SK+ (Stratagene) and sequenced. Relevant fragments (*Rsr*II-*Pfl*MI) from independent plasmids then replaced analogous fragment of pMwt, and one isolate was designated pMΔ86-106. Extensive resequencing confirmed that all plasmids were genetically identical to pMwt except for their PK_B and PK_C deletions. Each also contained the wild-type poly(C) tract. As with pMwt, the viral sequences were oriented in pBS (+/−) phagemid such that reactions with T7 RNA polymerase produced positive-sense, genomic-length transcripts containing 2 nonviral bases (GG) at the 5′ end and 7 nonviral bases (*Bam*HI site) linked to the 3′ poly$(A)_{23}$ tail (8, 18).

The viral cDNAs were linearized with *Bam*HI, reacted with T7 RNA polymerase (8), extracted with phenol-chloroform, and then precipitated with ethanol. Transcript length and homogeneity were confirmed by agarose electrophoresis before use in any experiments. Confluent HeLa cell monolayers in 60-mm plates were washed with phosphate-buffered saline (PBS) and Hanks' balanced salt solution (HBSS) and then exposed to lipofectin containing the appropriate RNA (0.004 to 1.5 μg) in HBSS (250 μl) (13). The cells were incubated under 0.8% agar at 37°C for 31 h under 5% CO_2 to allow for plaque development (24). Of the tested RNA transcripts, only those with deletions limited to PK_C gave plaques by this method (Table 1). The specific infectivity of pMΔ114, pMΔ114-119, and pMΔ107-139 transcripts was similar to that of the wild type ($\sim 10^{3.5}$ PFU per μg of RNA), but the plaques were uniformly smaller. Several independent plaques were picked for these PK_C isolates and then twice cloned before amplification into virus stocks. Reverse transcription PCR (RT-PCR) and dideoxy analysis of viral viral RNA (10), confirmed the deletion genotypes (genome bases 1 to 350), and further passage reaffirmed the plaque phenotypes. In a typical

TABLE 1. Pseudoknot mutant phenotypes[a]

RNA source	Putative effect of deletion	Specific infectivity (PFU/μg of RNA)	Plaque size[b]	No. of revertants isolated and their plaque sizes	Translation competence[c]
pMwt	Wild type	8.0×10^3	Medium	N/A	+++++
pMΔ86-106	Deletes PK_B	<0.33	Small	1 small	+++++
pMΔ114	Disrupts PK_C	4.3×10^3	Minute	3 small, 5 medium	+++++
pMΔ114-119	Disrupts PK_C	8.3×10^3	Minute	3 small	++++
pMΔ107-139	Deletes PK_C	6.8×10^3	Small	3 medium	+++++
pMΔ99-118	Disrupts PK_B and PK_C	0	N/A	0	++++
pMΔ90-144	Deletes PK_B and PK_C	0	N/A	0	++++
pMΔ56-134	Disrupts stem-loop A & deletes PK_B and PK_C	0	N/A	0	++++++

[a] Specific infectivity, plaque size, reversion propensity, and translation competence are shown for each mutant. All mutants were tested in parallel for each assay.
[b] As defined in reference 16: medium, ~2 to 3 mm; small, ~≤1 mm; minute, ≤0.5 mm. N/A, not available.
[c] Translation competence in rabbit reticulocyte lysates is indicated with plus symbols relative to pMwt. Each sign represents a 20% increment of acid-insoluble incorporation relative to pMwt (e.g., +++++ = 81 to 100%), as in reference 13.

plaque assay, virus diluted in PBS was attached to confluent HeLa cell monolayers for 30 min at room temperature. The plates were washed with PBS and then overlaid with medium containing 0.8% agarose (2.5 ml) and then with liquid medium (2.5 ml). The infected monolayers were incubated at 37°C for 30 h under a 5% CO_2 atmosphere and stained with crystal violet to visualize the plaques. Under these conditions, plaques created by mengovirus M or vMwt were of medium diameter (~3 mm) (16), but the 1-base and 6-base PK_C deletion sequences of vMΔ114 and vMΔ114-119 gave only tiny or minute-sized plaques (≤1.0 mm), indicating some sort of a replicative defect. The vMΔ107-139 stocks also gave small plaques (~1.5 mm) relative to vMwt, but these were discernibly larger than for the other PK_C deletions. The Δ107-139 deletion excised PK_C, while the other two deletions caused internal or local PK reconfiguration. The plaque sizes of these viruses suggested that partial disruption of this knot was somehow more debilitating to a basal function of the virus than specific knot excision.

All PK_C deletion isolates passaged with fidelity. Yet, after transfections with large doses of transcripts (as above, but with ≥3 μg of RNA and omitting the agar overlay) and subsequent passage of the resultant cellular extracts (three freeze-thaw cycles followed by low-speed clarification), each mutant also gave rise to occasional plaques that were distinctively larger than those of their parents (Table 1). Nine of these larger plaques were isolated and sequenced in the vicinity of the 5′ terminus (viral bases 1 to 350). None was found to carry new alterations or offsetting pseudoknot changes in the surrounding 5′ region, leading to the conclusion that second-site reversions must lie elsewhere in these genomes and which compensated, in part, for the functional defects conferred by the pseudoknot deletions. Recombinant analyses to identify the relevant loci are currently under way.

In contrast to the PK_C sequences, none of the tested deletions that impinged on PK_B were infectious. Even the precise deletion of this knot (pMΔ86-106) was lethal. Forced passage of the transfected cell lysates (3 μg of RNA per plate), after freeze-thaw and clarification, did eventually give one small plaque for the Δ86-106 sequence, but the same procedure did not give plaques for any of the other related PK_B mutations. This single PK_B isolate was presumed to be a revertant because it passaged easily when replated. The genomic sequence of this putative revertant has not yet been analyzed.

The growth properties of many picornaviruses are known to be sensitive to variable incubation temperatures. Accordingly, the viable pseudoknot mutants were tested at higher (39°C) and lower (33°C) growth temperatures than normal (37°C). Mengoviruses M, vMwt, vMΔ114, vMΔ114-119, and vMΔ107-139 titered with the same plating efficiencies at all temperatures. Typical of most viruses, their plaques were larger at 39°C and smaller at 33°C than at 37°C, but the variation was coordinate among all strains and no mutant showed a clearly enhanced heat or cold sensitivity relative to normal mengovirus (not shown). But, for a plaque to develop, multiple rounds of infection must occur, thus providing opportunity to magnify genetic defects and/or cellular responses that may influence viral growth. To better characterize the growth defects in the viable PK_C mutants, the single-step growth kinetics were measured after synchronized infection of HeLa cells (Fig. 2). The

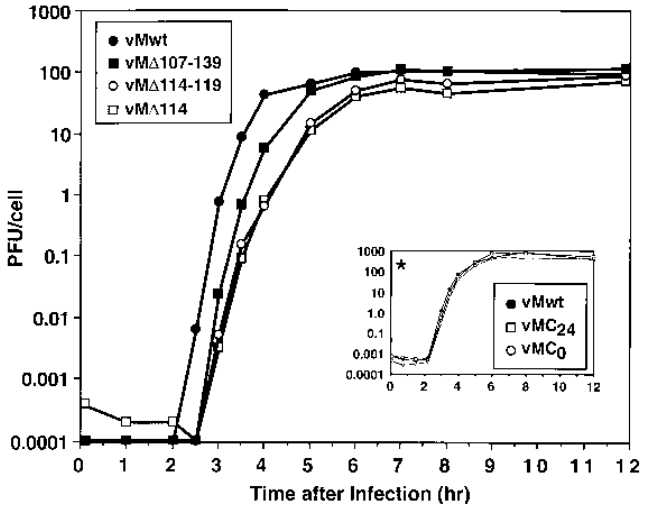

FIG. 2. Single-step growth. Virus attachment to HeLa cells was carried out in suspension cultures (6×10^7 cells, 10 PFU per cell) for 30 min at room temperature (25°C), and unattached infectivity was removed by rinsing and low-speed centrifugation. Cultures were reconstituted in minimal essential medium before transfer to a 37°C shaking water bath (zero hour time point). Culture aliquots were removed at indicated times and freeze-thawed three times, and virus titers were determined by plaque assay (10). The data are plotted as PFU per cell. For comparison, the inset shows an analogous experiment from reference 16 with vMC_0, vMC_{24}, and vMwt mengoviruses with poly(C) tract sequences of C_0, C_{24}, and $C_{44}UC_{10}$, respectively.

three mutants all emerged from eclipse about 0.5 h later than vMwt, indicating their disrupted pseudoknots had an effect early in infection. During the exponential growth phase, each mutant then showed a rate of amplification consistent with its relative plaque size: vMΔ107-139 grew faster and to a higher titer than vMΔ114 or vMΔ114-119. This again suggests their deficiencies were expressed continuously through the growth cycle and, moreover, that deletion of PK_C, rather than its disruption, was more easily tolerated. By 12 h postinoculation, all mutant titers had increased to the level of vMwt.

The viral poly(C) tract 3′ to PK_B and PK_C plays a significant role in mengovirus virulence (7, 20). Normally, an infection with wild-type virus causes a rapid, lethal meningoencephalomyelitis in many types of animals, including rodents, pigs, and primates (18). However, genetically engineered short poly(C) viruses, such as vMC_0 and vMC_{24}, have median 50% lethal dose values (LD_{50}s) in mice that are at least 10^6-fold higher than those for vMwt or M, although these viruses differ only in the absolute length of this tract (16). To assess whether the pseudoknots work in concert with the poly(C) to mediate mengovirus virulence, the LD_{50} of the most vigorously growing PK_C deletion was determined in Swiss/ICR mice. Four groups of five mice each were inoculated intracerebrally with incremental doses of virus, and lethality was assessed over a 2-week period (7). Upon death, replicate virus isolates were recovered from brain homogenates and analyzed for plaque phenotype and also for 5′ UTR genotype by RT-PCR and dideoxy sequencing. Only the parental, inoculated viruses were recovered. The LD_{50} of vMΔ107-139 was measured at $10^{4.4}$ PFU. The LD_{50} for vMwt in a parallel assay was $10^{3.3}$ PFU. Thus, the PK_C deletion increased the LD_{50}, relative to vMwt by ~10-fold, which is much lower than that achieved by nearby poly(C) deletions (16) and not more than might be expected for any virus with a somewhat reduced plaqueing vigor. Since mutations in this pseudoknot did not behave like a coordinate extension of the poly(C) region, either in tissue culture or in mice, we conclude that the biological functions of PK_C, and by inference its neighbor PK_B, are probably unrelated to the poly(C) attenuation phenomenon.

Why then, are the pseudoknots present in these viruses? In addition to the poly(C)-dependent virulence activities, the mengovirus 5′ UTR harbors other mapped translational and replication regulatory features. An uncommonly effective, internal ribosome entry site (IRES), for example, mediates the initiation of genome translation (6). The required 450-base segment is located 5′ to the polyprotein initiation codon (mengovirus bases 753-755), and about 200 bases 3′ to the pseudoknots (6). Recombinant mapping experiments with monocistronic and dicistronic mRNAs have usually focused on the IRES element itself, and it has been assumed, but never tested, that upstream structural units, like the pseudoknots, would have little impact on polyprotein translation. To confirm this assumption, full-length transcripts from pMwt, pMΔ114, pMΔ114-119, and pMΔ107-139 cDNAs were used to program cell-free translation reactions in reticulocyte lysates. The relative incorporation of ^{35}S-methionine was similar for all sequences (Table 1) and within ranges consistent for analogous comparative translational assays (12). This indicates that the pseudoknot region, as expected, was functionally invisible to ribosomes, at least in cell-free extracts, and translational regulatory roles are probably not vested in this area.

Instead, the absolute lethality of the PK_B and PK_B+PK_C deletions, and their relative positions near the 5′ terminus of the genome, alternatively suggested these motifs might play a role in viral RNA replication. Indeed, by analogy with a 5′ terminal cloverleaf structure in poliovirus, the mengovirus 5′ stem-loop A has been proposed as a recognition element in the RNA synthesis pathway (2, 23). Accordingly, HeLa cells were infected with vMwt or with the viable mutants and then monitored for [^{3}H]-uridine incorporation after treatment with actinomycin D (Fig. 3). All three mutants (vMΔ114, vMΔ114-119, and vMΔ107-139) were much less efficient than vMwt at directing label incorporation, accumulating only ~10% as much RNA within the 8-h assay. Unfortunately, only those mutations constrained to PK_C could be tested in this assay, because the other deletions, impinging on PK_B, were lethal and did not produce virus. Still, the incorporation values were consistent with the observed decrease in viral replication in the growth experiments and plaque assays and imply the pseudoknots contribute in a vital way to viral RNA synthesis. The general inability to force even (pseudo)reversions for most of the PK_B deletions is also consistent with this notion and even expected for debilitating defects in the RNA synthesis pathways. Mutational rescue or fixation of reversions can happen efficiently only when replication is occurring. We propose that both of these knots, and presumably those equivalently arrayed in other picornaviruses, provide some critical recognition or mechanistic links that are required for genomic amplification.

That PK_C deletion sequences were not crippled to the same extent as those carrying deletions in both knots simultaneously, or to PK_B alone, suggests that PK_B may be functionally dominant to PK_C, but for reasons that remain unclear. PK_B could easily be modeled as a quasicontinuous stacked helix, coaxial with the base of stem-loop A (26). Thus, PK_B and also PK_C could be visualized as terminal extensions of this structure. Such a complex would bring the knots into physical proximity with VPg, the small, virally encoded, genome-linked protein attached by a tyrosine-O^4-phosphodiester bond to the 5′ terminal uridine nucleotide of the genome (27). VPg addition or its recognition is an essential step in the initiation of RNA synthesis (5). Work with the analogous 5′ terminal cloverleaf

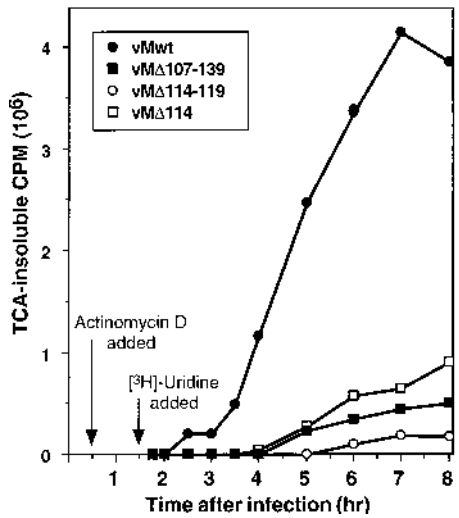

FIG. 3. [^{3}H]Uridine incorporation. Single-step growth experiments were similar to those described in the legend to Fig. 2, except at 30 min postattachment, 5 μg of actinomycin D (Sigma) per ml was added, and at 1.5 h postattachment, 1 mCi of [^{3}H]uridine (Amersham) per ml was added per 10^8 cells. At the indicated times, 10-μl aliquots were streaked in duplicate onto Casamino acid-sodium dodecyl sulfate-treated cellulose filter papers (Whatman) and washed, and resultant, trichloroacetic acid-insoluble radioactivity was measured by scintillation counting (21). Parallel, mock-infected cultures measured background incorporation.

of poliovirus (1) has revealed that a functional ribonucleoprotein complex, including at least two viral proteins and a host factor, does indeed form around this region and plays an important though undefined role in replication (2, 11, 23). If the cardiovirus stemloop A and its associated pseudoknots function in a similar manner, the behavior of our mutants becomes more understandable. Studies are now under way to quantitate the accumulation of both plus and minus strands in mutant PK_C-infected cells and also in cells transfected with the PK_B sequences. We intend also to complete the pseudoreversion mapping in the expectation of identifying viral protein segments that may interact with this region. We hope such data will point to a more specific role for these knotted structures in the viral life cycle.

This work was supported by National Institutes of Health Grant AI-30566 to A.C.P. and NIH Training Grant GM-07215 to L.R.M.

We thank the members of the Palmenberg and Roland Rueckert laboratories for their insightful and critical evaluation of this work, and we specifically thank Marchel Hill and Jim Schrader for valuable technical assistance.

REFERENCES

1. **Andino, R., G. E. Rieckhof, P. L. Achacoso, and D. Baltimore.** 1993. Poliovirus RNA synthesis utilizes an RNP complex formed around the 5′-end of viral RNA. EMBO J. **12:**3587–3598.
2. **Andino, R., G. E. Rieckhof, and D. Baltimore.** 1990. A functional ribonucleoprotein complex forms around the 5′ end of poliovirus RNA. Cell **63:**369–380.
3. **Baltimore, D., R. N. Franklin, H. J. Eggers, and I. Tamm.** 1963. Poliovirus induced RNA polymerase and the effects of virus-specific inhibitors on its production. Proc. Natl. Acad. Sci. USA **49:**843–849.
4. **Clarke, B. E., A. L. Brown, K. M. Curry, S. E. Newton, D. J. Rowlands, and A. R. Carroll.** 1987. Potential secondary and tertiary structure in the genomic RNA of foot-and-mouth disease virus. Nucleic Acids Res. **15:**7067–7079.
5. **Crawford, N. M., and D. Baltimore.** 1983. Genome-linked protein VPg of poliovirus present as VPg and VPg-pUpU in poliovirus-infected cells. Proc. Natl. Acad. Sci. USA **80:**7452–7455.
6. **Duke, G. M., M. A. Hoffman, and A. C. Palmenberg.** 1992. Sequence and structural elements that contribute to efficient encephalomyocarditis viral RNA translation. J. Virol. **66:**1602–1609.
7. **Duke, G. M., J. E. Osorio, and A. C. Palmenberg.** 1990. Attenuation of mengovirus through genetic engineering of the 5′ noncoding poly(C) tract. Nature (London) **343:**474–476.
8. **Duke, G. M., and A. C. Palmenberg.** 1989. Cloning and synthesis of infectious cardiovirus RNAs containing short, discrete poly(C) tracts. J. Virol. **63:**1822–1826.
9. **Escarmis, C., M. Toja, M. Medina, and E. Domingo.** 1992. Modifications of the 5′ untranslated region of foot-and-mouth disease virus after prolonged persistence in cell culture. Virus Res. **26:**113–125.
10. **Hahn, H., and A. C. Palmenberg.** 1995. Encephalomyocarditis viruses with short poly(C) tracts are more virulent than their mengovirus counterparts. J. Virol. **69:**2697–2699.
11. **Harris, K. S., W. Xiang, L. Alexander, A. V. Paul, W. S. Lane, and E. Wimmer.** 1994. Interaction of the poliovirus polypeptide $3CD^{pro}$ with the 5′ and 3′ termini of the poliovirus genome: identification of viral and cellular cofactors necessary for efficient binding. J. Biol. Chem. **269:**27004–27014.
12. **Hoffman, M. A., and A. C. Palmenberg.** 1995. Mutational analysis of the J-K stem-loop region of the encephalomyocarditis virus IRES. J. Virol. **69:**4399–4406.
13. **Hoffman, M. A., and A. C. Palmenberg.** 1996. Revertant analysis of J-K stem-loop mutations in the encephalomyocarditis virus IRES detects an altered leader protein. J. Virol. **70:**6425–6430.
14. **Jayaraman, K., and C. J. Puccini.** 1992. A PCR-mediated gene synthesis strategy involving the assembly of oligonucleotides representing only one of the strands. BioTechniques **12:**392–398.
15. **Le, S. Y., J. H. Chen, N. Sonenberg, and J. V. Maizel.** 1993. Conserved tertiary structural elements in the 5′ nontranslated region of cardiovirus, apthovirus and hepatitis A virus RNAs. Nucleic Acids Res. **21:**2445–2451.
16. **Martin, L. R., G. M. Duke, J. E. Osorio, and A. C. Palmenberg.** 1996. Mutational analysis of the mengovirus poly(C) tract and surrounding heteropolymeric sequences. J. Virol. **70:**2027–2031.
17. **Najarian, R., D. Caput, W. Gee, S. Potter, A. Renard, J. Merryweather, G. Van Nest, and D. Dina.** 1985. Primary structure and gene organization of human hepatitis A virus. Proc. Natl. Acad. Sci. USA **82:**2627–2631.
18. **Osorio, J. E., G. B. Hubbard, K. F. Soike, M. Girard, S. van der Werf, and A. C. Palmenberg.** 1996. Protection of non-murine mammals against encephalomycarditis using a genetically engineered mengo virus. Vaccine **14:**155–161.
19. **Palmenberg, A. C.** 1987. Comparative organization and genome structure in picornaviruses, p. 25–34. *In* M. A. Brinton and R. R. Rueckert (ed.), Positive strand RNA viruses. Alan R. Liss Press, New York.
20. **Palmenberg, A. C., and J. E. Osorio.** 1994. Cardioviral poly(C) tracts and viral pathogenesis. Arch. Virol. **90:**67–77.
21. **Palmenberg, A. C., M. A. Pallansch, and R. R. Rueckert.** 1979. Protease required for processing picornaviral coat protein resides in the viral replicase gene. J. Virol. **32:**770–778.
22. **Rieder, E., T. Bunch, F. Brown, and P. W. Mason.** 1993. Genetically engineered foot-and-mouth disease viruses with poly(C) tracts of two nucleotides are virulent in mice. J. Virol. **67:**5139–5145.
23. **Rohll, J. B., N. Percy, R. Ley, D. J. Evans, J. W. Almond, and W. S. Barclay.** 1994. The 5′-untranslated regions of picornavirus RNAs contain independent functional domains essential for RNA replication and translation. J. Virol. **68:**4384–4391.
24. **Rueckert, R. R., and M. A. Pallansch.** 1981. Preparation and characterization of encephalomyocarditis virus. Methods Enzymol. **78:**315–325.
25. **Sandhu, G. S., R. A. Aleff, and B. C. Kline.** 1992. Dual asymmetric PCR: one-step construction of synthetic genes. BioTechniques **12:**14–16.

25a. **Sgro, J. Y., and A. C. Palmenberg.** Unpublished data.

26. **ten Dam, E., K. Pleij, and D. Draper.** 1992. Structural and functional aspects of RNA pseudoknots. Biochemistry **31:**11667–11676.
27. **Vartapetian, A. B., E. V. Koonin, V. I. Agol, and A. A. Bogdanov.** 1984. Encephalomyocarditis virus RNA synthesis in vitro is protein-primed. EMBO J. **3:**2593–2598.
28. **Vartapetian, A. B., A. S. Mankin, E. V. Shripkin, K. M. Chumakov, V. D. Smirnov, and A. A. Bogdanov.** 1983. The primary and secondary structure of the 5′ end region of encephalomyocarditis virus RNA. A novel approach to sequencing long RNA molecules. Gene **26:**189–195.